International Journal of Control, Automation and Systems VV(N) (YYYY) 1-3
http://dx.doi.org/10.1007/s12555-015-0192-y
ISSN:1598-6446 eISSN:2005-4092
http://www.springer.com/12555

Time-Optimal Velocity Planning Along Predefined Path for Static Formations of Mobile Robots

Toni Petrinić*, Mišel Brezak, and Ivan Petrović

Abstract: This paper is concerned with the problem of finding a time-optimal velocity profile along the predefined path for static formations of mobile robots in order to traverse the path in shortest time and to satisfy, for each mobile robot in the formation, velocity, acceleration, tip over and wheel slip prevention constraints. Time-optimal velocity planning is achieved using so called bang-bang control where minimum and maximum accelerations of the formation are alternating. The developed trajectory planning algorithm is demonstrated on the formation of differential drive mobile robots.

Keywords: differential drive mobile robot, mobile robot formations, velocity and acceleration constraints, tip over and wheel slip prevention, trajectory planning

1. INTRODUCTION

Research interest in systems with multiple robots has recently grown enormously in the control community. The usage of multiple robots has several advantages compared to a single robot. For example, multiple robots may be able to achieve tasks that are impossible for a single robot. Also, multiple robots are more robust to failure than a single robot (one robot can take over the tasks of another robot in case of failure). Since robots can have a variety of roles, the same group of robots can be employed for many different objectives, e.g. optimal area coverage for mapping and exploration, cooperative transportation, cooperative harvesting, cooperative snow removal, etc. The ability to maintain a formation, i.e. a specified spatial relationship between members of the group during group motion through a workspace, is a fundamental requirement for any multi-robot system.

This paper investigates the time-optimal motion of the static formation of mobile robots along predefined collision-free path. If we treat the formation of mobile robots as one multi-body robot, many of existing single-robot algorithms can be used to find collision-free path, e.g. [1-3], and to smooth path, e.g. [4]. Also, the user can manually specify the collision-free path. Existing single-robot motion planners can be adapted to plan the velocity profile of the formation of mobile robots. Then for each mobile robot in the formation it is possible to compute individual velocity profile based on the planned velocity of the entire formation. This is similar to the leader-follower approach [5].

The algorithm that solves the problem of moving a manipulator in time-optimal (minimum-time) along a specified geometric path subject to input torque/force is described in [6, 7]. The power of that algorithm lies in its generality as it can be used with variety of constraints. Moreover, it can be adapted for planning of time-optimal trajectory for the formation of mobile robots satisfying complex constraints of each mobile robot in the formation. In [8] is presented a newer discrete version of algorithm [6, 7] that gives near time-optimal solution.

Time-optimal velocity planning along predefined path for one mobile robot is well researched. Planning the time-optimal velocity considering velocity and acceleration constraints is described in [9, 10], and with jerk constraints in [11]. Some researchers go one step further and take additionally into account tip over and wheel slip prevention constraints [12-14]. In [15], visibility constraint is taken into account by mapping the Euclidean homography matrix to the image space. Maximum vehicle speed due to comfort and safety reasons are expressed via lateral acceleration in [16].

To plan trajectory for the formation of mobile robots, researchers typically take into account only velocity and curvature constraints of each robot [17-19]. However, the problem of time-optimal velocity planning for the formation of mobile robots is still an open research problem. By extending approach [12] to the static formation of mobile robots, to the best of our knowledge, we are the first who compute time-optimal velocity profile along the smooth predefined path for static formations of mobile robots.

Manuscript received May 03, 2015; revised November 30, 2015; accepted January 28, 2016. Recommended by Editor Hyouk Ryeol Choi.
Toni Petrinić is with the HEP-ODS d.o.o., Elektroprimorje Rijeka, Pogon Cres-Lošinj, Dražica 10, 51550 Mali Lošinj, Croatia (e-mail: toni.petrinic@gmail.com).
Mišel Brezak is with the Polytechnic Hrvatsko Zagorje Krapina, Šetalište Hrvatskog narodnog preporoda 6, 49000 Krapina, Croatia (e-mail: misel.brezak@gmail.com).
Ivan Petrović is with the University of Zagreb, Faculty of Electrical Engineering and Computing, Unska 3, 10000 Zagreb, Croatia (e-mail: ivan.petrovic@fer.hr).
* Corresponding author.

ICROS, KIEE and Springer 2016

The rest of the paper is organized as follows. In Section 2 static formations of mobile robots are described. In Section 3 a dynamic model of differential-drive mobile robot that accounts for velocity, acceleration, tip over and wheel slip prevention constraints is shortly presented and utilized for time-optimal velocity planning algorithm. A time-optimal velocity planning algorithm for static formations of mobile robots is derived in Section 4. Experimental results are presented in Section 5. The paper ends with the conclusion.

2. STATIC FORMATIONS OF MOBILE ROBOTS

In the proposed approach, the user first defines a reference point, which is an arbitrary point C within the formation whose coordinates serve as reference coordinates for the group of mobile robots. The reference point C is usually at the location of one of the mobile robots in the formation. A reference path is the path of the reference point C. Positions of all mobile robots in the formation are given relative to this reference point (Fig. 1). The coordinates of the i-th mobile robot relative to the reference point C are denoted as (p^i, r^i), where p^i is the distance along the reference path and r^i is the distance in the perpendicular direction relative to the tangent of the reference path (so called curvilinear coordinates). By static formation we mean that p^i and r^i are constant.

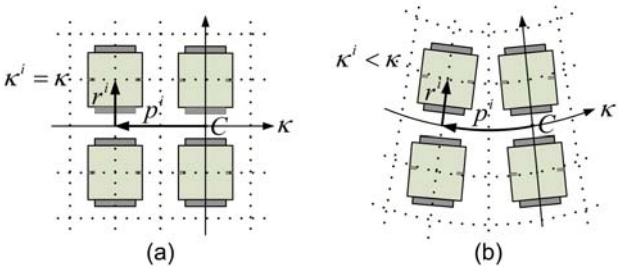

Fig. 1. a) Square formation in straigt line, b) square formation in the curve.

The shape of a formation, as defined above, will slightly alter while turning, as depicted in Fig 1. b). Thus, the formation is not rigid but flexible, which is appropriate for tasks such as harvesting, snow removal or mapping and exploration tasks where a particular offset between robots is required to ensure accurate data.

In this work we assume that the formation reference path consists of lines and clothoids, but any other curve types can be used. Clothoids [20] are used due to their attractive property of linear relation between the curvature and the arc length. Thus produced reference path is G^2 continuous and, as the offset of the clothoid is also G^2 continuous, paths of all the robots in the formation will be G^2 continuous, too.

We deal with the differential-drive mobile robot whose kinematic model is given by

$$\begin{bmatrix} \dot{x}(t) \\ \dot{y}(t) \\ \dot{\theta}(t) \end{bmatrix} = \begin{bmatrix} cos\theta(t) & 0 \\ sin\theta(t) & 0 \\ 0 & 1 \end{bmatrix} \cdot \begin{bmatrix} v(t) \\ \omega(t) \end{bmatrix}, \tag{1}$$

where t is time, $(x(t), y(t))$ position, $\theta(t)$ orientation, and $v(t)$ and $\omega(t)$ longitudinal and angular velocity of the mobile robot, respectively.

The nonholonomic constraint of the system (1) is

$$-\dot{x}(t) \cdot \sin\theta(t) + \dot{y}(t) \cdot \sin\theta(t) = 0, \tag{2}$$

which represents unrealizable sideway motion.

We suppose that the reference path of the formation $q(s) = [x(s) \;\; y(s) \;\; \theta(s)]^T$ is known in advance, where path parameter s denotes the distance travelled along the path. Let $q^i(s)$ denote path, $\kappa^i(s)$ path curvature and $s^i(s)$ travelled distance of the i-th mobile robot in the formation. If $\kappa(s)$ is reference path curvature, path curvature and its derivative for i-th mobile robot can be calculated as (Fig. 2):

$$\kappa^i(s) = \frac{\kappa(s + p^i)}{1 - r^i \cdot \kappa(s + p^i)}, \tag{3}$$

$$\frac{d\kappa^i(s)}{ds} = \frac{\dfrac{d\kappa(s + p^i)}{ds}}{\left[1 - r^i \cdot \kappa(s + p^i)\right]^2}. \tag{4}$$

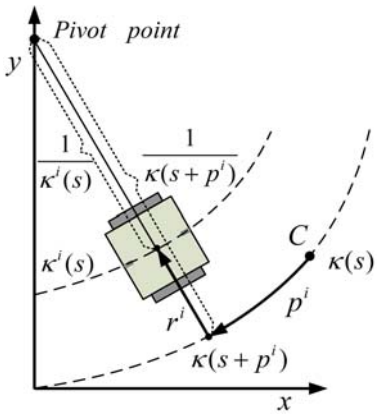

Fig. 2. Path curvature.

If $1 - r^i \cdot \kappa(s + p^i) = 0$, the i-th mobile robot is positioned exactly at the center of curvature of the reference trajectory whereupon (3) and (4) are infinite while mobile robot longitudinal velocity is zero as will be shown later in Section 4. Infinite path curvature implies that the mobile robot must turn on the spot to maintain formation which is possible for differential drive robots. While it is easy to derive necessary relationships between reference path and its offset for the straight line segments of the reference path, for the clothoid segments it is quite complicated. In the continuation we derive the equation for the clothoid, which is required for further discussion. For simplicity let $p^i = 0$ (Fig. 2).

Basic parametric equation of the clothoid curve with zero initial curvature is

$$\begin{bmatrix} x_c(s) \\ y_c(s) \end{bmatrix} = \int_0^s \begin{bmatrix} \cos(0.5 \cdot \xi^2 \cdot \sigma) \\ \sin(0.5 \cdot \xi^2 \cdot \sigma) \end{bmatrix} d\xi, \tag{5}$$

where σ is parameter called sharpness of the clothoid. The curvature of the clothoid curve changes linearly with its arc length

$$\kappa(s) = \sigma \cdot s. \tag{6}$$

The offset of parametrically defined curve with constant distance r^i along the perpendicular direction in the general case is given by [21]

$$\begin{bmatrix} x_{off}(s) \\ y_{off}(s) \end{bmatrix} = \begin{bmatrix} x(s) \\ y(s) \end{bmatrix} + \frac{r^i}{\sqrt{\left(\frac{dx(s)}{ds}\right)^2 + \left(\frac{dy(s)}{ds}\right)^2}} \cdot \begin{bmatrix} -\frac{dy(s)}{ds} \\ \frac{dx(s)}{ds} \end{bmatrix}. \tag{7}$$

By substituting (5) into (7) we obtain clothoid offset

$$\begin{bmatrix} x_{c,off}(s) \\ y_{c,off}(s) \end{bmatrix} = \int_0^s \begin{bmatrix} \cos\left(0.5 \cdot \xi^2 \cdot \sigma\right) \\ \sin\left(0.5 \cdot \xi^2 \cdot \sigma\right) \end{bmatrix} d\xi + r^i \cdot \begin{bmatrix} -\sin\left(0.5 \cdot s^2 \cdot \sigma\right) \\ \cos\left(0.5 \cdot s^2 \cdot \sigma\right) \end{bmatrix}. \tag{8}$$

For further discussion we differentiate (8):

$$\begin{bmatrix} dx_{c,off}(s) \\ dy_{c,off}(s) \end{bmatrix} = \left(\begin{bmatrix} \cos\left(0.5 \cdot s^2 \cdot \sigma\right) \\ \sin\left(0.5 \cdot s^2 \cdot \sigma\right) \end{bmatrix} - r^i \cdot \kappa(s) \cdot \begin{bmatrix} \cos\left(0.5 \cdot s^2 \cdot \sigma\right) \\ \sin\left(0.5 \cdot s^2 \cdot \sigma\right) \end{bmatrix} \right) ds. \tag{9}$$

Using (9) we obtain arc length of clothoid offset s^i with respect to arc length of the clothoid s

$$ds^i(s) = \sqrt{dx_{c,off}(s)^2 + dy_{c,off}(s)^2}\, ds = = \left|1 - r^i \cdot \kappa(s)\right| ds. \tag{10}$$

Note that for the line it is $\kappa(s) = 0$ so that $ds^i(s) = ds$.

3. DYNAMIC MODEL OF DIFFERENTIAL-DRIVE MOBILE ROBOT FOR TIME-OPTIMAL VELOCITY PLANNING ALGOTIHM

3.1. Derivation of the dynamic model

Let's assume that a reference collision-free path $q(s)$ is a twice-differentiable curve, i.e. G^2 continuous, in the configuration space $q(s):[0,s_g] \to CS$, which maps a path parameter s to a curve in configuration space CS, where s_g is path parameter at the goal. A trajectory is specified by a time-scaling function $s(t):[0,t_g] \to [0,s_g]$, which assigns a value s to each time $t \in [0,t_g]$. The time-scaling function $s(t)$ is assumed to be twice-differentiable and monotonic, i.e. $\dot{s}(t) > 0$, where $\dot{s}(t)$ denotes time derivative of $s(t)$. Using both path and time scaling, a trajectory can now be defined as $q(s(t)):[0,t_g] \to CS$, which is short-written as $q(t)$.

Let a general dynamic model of the robot be given by

$$u = M(q) \cdot \ddot{q} + \dot{q}^T \cdot \Gamma(q) \cdot \dot{q} + g(q), \tag{11}$$

where u is the vector of generalized forces acting on the generalized coordinates q, $M(q)$ is a mass or inertia matrix, $\Gamma(q)$ can be viewed as an vector, where each element is a matrix whose elements are Christoffel symbols of the inertia matrix and $g(q)$ is a vector of gravitational forces.

The developed forces in (11) are subject to the actuator lower and upper limits and in the most general form are expressed as functions of the robot configuration and velocity

$$u_j^{min}(q,\dot{q}) \le u_j \le u_j^{max}(q,\dot{q}). \tag{12}$$

By expressing the path q as a function of parameter s, (11) can be written as the vector equation

$$a(s) \cdot \ddot{s} + b(s) \cdot \dot{s}^2 + c(s) = u, \tag{13}$$

which defines robot dynamic model constrained to the path $q(s)$. The vector functions $a(s)$, $b(s)$ and $c(s)$ are inertial, velocity product and gravitational terms, respectively.

Because the robot motion is constrained to the path, its state at any time is determined by $(s,\dot{s})$ and actuator limits can be expressed as a function of $(s,\dot{s})$. From (13), it may be concluded that the system must satisfy

$$u^{min}(s,\dot{s}) \le a(s) \cdot \ddot{s} + b(s) \cdot \dot{s}^2 + c(s) \le u^{max}(s,\dot{s}). \tag{14}$$

This equation enables us to express the minimum and maximum accelerations $\ddot{s}$ as functions of $(s,\dot{s})$, which are required to obtain time-optimal scaling function. We denote the minimum and maximum accelerations $\ddot{s}$ satisfying the j-th component of (14) by $L_j(s,\dot{s})$ and $U_j(s,\dot{s})$, respectively.

We define overall acceleration limits as

$$L(s,\dot{s}) = \max_{j=1,\ldots,n_c} L_j(s,\dot{s}), \quad U(s,\dot{s}) = \min_{j=1,\ldots,n_c} U_j(s,\dot{s}), \tag{15}$$

where n_c is the total number of mobile robot acceleration limits.

The acceleration limits (14) can now simply be expressed as

$$L(s,\dot{s}) \le \ddot{s} \le U(s,\dot{s}). \tag{16}$$

We use longitudinal acceleration a and angular acceleration α as generalized forces, i.e. as the command input in model (11),

$$u = \begin{bmatrix} a & \alpha \end{bmatrix}^T. \tag{17}$$

These accelerations are proportional to the corresponding forces. Although the vector u does not give robot configuration (i.e. position and orientation) directly, the trajectory planning will yield the time-scaling function $\dot{s}(t)$ which we integrate to obtain $s(t)$ and then configuration $q(t)$ is computed by substituting $s(t)$ into the predefined path $q(s)$.

We choose that the path parameter s denotes the distance travelled along the path in the case that robot motion has translation component. In that case longitudinal velocity $v(t)$ is non-zero and under assumption that path curvature $\kappa(s)$ is continuous, longitudinal velocity and angular velocity can be expressed as function of s

$$v(t) = \dot{s}(t), \quad \omega(t) = \kappa(s(t)) \cdot \dot{s}(t). \tag{18}$$

By differentiating (18), we obtain accelerations

$$\begin{aligned} a(t) &= \dot{v}(t) = \ddot{s}(t), \\ \alpha(t) &= \dot{\omega}(t) = \kappa(s(t)) \cdot \ddot{s}(t) + \frac{d\kappa(t)}{ds} \cdot \dot{s}(t)^2. \end{aligned} \tag{19}$$

Substitution of (19) into (17) gives dynamic model of differential drive mobile robot

$$\begin{bmatrix} 1 \\ \kappa(s) \end{bmatrix} \cdot \ddot{s} + \begin{bmatrix} 0 \\ \dfrac{d\kappa(s)}{ds} \end{bmatrix} \cdot \dot{s}^2 = \begin{bmatrix} a \\ \alpha \end{bmatrix}. \tag{20}$$

3.2. Derivation of acceleration limits

Motion of a mobile robot is affected by various forces (gravity, centrifugal force and centripetal force). These forces contribute to dynamic problems such as the slip and over-actuation of wheels, limitations of velocity and acceleration, and the effects of inertia. To make the paper self-contained we give a short description of acceleration limits (16) considering velocity, acceleration and wheel slip prevention constraints, while detailed description can be found in [12].

Let $\bar{a}_{\min}$ be a negative constant denoting minimum longitudinal acceleration, $\bar{a}_{\max}$ a positive constant denoting maximum longitudinal acceleration, $\bar{v}_{\max}$ maximum absolute longitudinal velocity of the robot, $\bar{\alpha}_{\min}$ a negative constant denoting minimum angular acceleration, $\bar{\alpha}_{\max}$ a positive constant denoting maximum angular acceleration and $\bar{\omega}_{\max}$ maximum absolute angular velocity of the robot.

From the robot dynamic model (20), acceleration constraints due to limited longitudinal acceleration is

$$\begin{aligned} &L_1(s,\dot{s}) = a_{min}(s,\dot{s}), \;\; U_1(s,\dot{s}) = a_{max}(s,\dot{s}), \\ &a_{min}(s,\dot{s}) = \begin{cases} \bar{a}_{min}, & \dot{s} \in (-\bar{v}_{max}, \bar{v}_{max}) \\ 0, & otherwise \end{cases}, \\ &a_{\max}(s,\dot{s}) = \begin{cases} \bar{a}_{\max}, & \dot{s} \in (-\bar{v}_{max}, \bar{v}_{max}) \\ 0, & otherwise \end{cases}, \end{aligned} \tag{21}$$

and due to limited angular acceleration is

$$\begin{bmatrix} L_2(s,\dot{s}) \\ U_2(s,\dot{s}) \end{bmatrix} = \begin{cases} \dfrac{\begin{bmatrix} \alpha_{min}(s,\dot{s}) \\ \alpha_{max}(s,\dot{s}) \end{bmatrix} - \dfrac{d\kappa(s)}{ds} \cdot \dot{s}^2}{\kappa(s)}, & \kappa(s) > 0 \\ \text{undefined}, & \kappa(s) = 0, \\ \dfrac{\begin{bmatrix} \alpha_{max}(s,\dot{s}) \\ \alpha_{min}(s,\dot{s}) \end{bmatrix} - \dfrac{d\kappa(s)}{ds} \cdot \dot{s}^2}{\kappa(s)}, & \kappa(s) < 0 \end{cases}$$

$$\alpha_{min}(s,\dot{s}) = \begin{cases} \bar{\alpha}_{min}, & \kappa(s) = 0 \vee \dot{s} \in \left[\dfrac{-\bar{\omega}_{max}}{|\kappa(s)|}, \dfrac{\bar{\omega}_{max}}{|\kappa(s)|} \right] \\ 0, & \text{otherwise} \end{cases},$$

$$\alpha_{\max}(s,\dot{s}) = \begin{cases} \bar{\alpha}_{\max}, & \kappa(s) = 0 \vee \dot{s} \in \left[\dfrac{-\bar{\omega}_{max}}{|\kappa(s)|}, \dfrac{\bar{\omega}_{max}}{|\kappa(s)|} \right] \\ 0, & \text{otherwise} \end{cases}, \tag{22}$$

For $\kappa(s) = 0$ (22) is undefined because pure translation is not constrained by angular acceleration limit.

To prevent slip of the robot wheels we have to ensure that required overall forces on the wheels F_k do not exceed maximum available friction forces between the wheels and the ground $F_{fr,\mathrm{k}}$, i.e.

$$F_k \le F_{fr,\mathrm{k}}, \tag{23}$$

where $k = 1$ for the left, and $k = 2$ for the right wheel.

The force on each wheel consists of a longitudinal and a lateral component (Fig. 3(a)). The longitudinal component comes from the torque used to accelerate or decelerate wheels. The lateral component develops if the robot translates and rotates at the same time and is caused by inertial centrifugal force. Each wheel takes the half of the total centrifugal force. The overall force developed on each wheel is

$$\begin{aligned} F_k^2 &= F_{long,\mathrm{k}}^2 + \frac{F_{cf}^2}{4}, \\ F_{long,k} &= \frac{m}{2} \cdot \dot{v} - \lambda \cdot \frac{J}{d_w} \cdot \dot{\omega}, \\ F_{cf} &= m \cdot a_{cf} = m \cdot v \cdot \omega, \end{aligned} \tag{24}$$

where $F_{long,\mathrm{k}}$ is the longitudinal force component, F_{cf} is the overall centrifugal force acting on the robot, m and J are the mass and the inertia of the robot, respectively, d_w is the distance between driving wheels,

a_{cf} is the centrifugal force, $\lambda = 1$ for the left and $\lambda = -1$ for the right wheel.

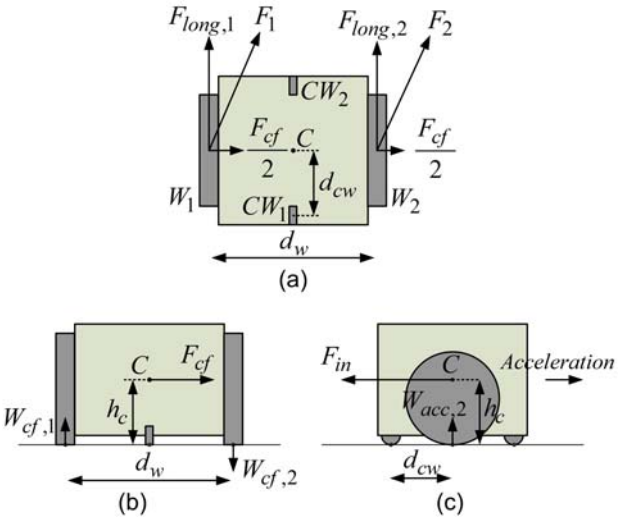

Fig. 3. a) Top view of the robot, b) rear view of the robot, c) side view of the robot.

To express friction forces, the Coulomb's friction model is used. A prerequisite for the Coulomb's model application is to compute overall weighting forces on each wheel W_k (Fig. 3(b) and Fig. 3(c)),

$$\begin{aligned} W_k &= W_{static} + W_{cf,\mathrm{k}} + W_{acc,\mathrm{k}}, \\ W_{static} &= m \cdot \frac{g}{2}, \\ W_{cf,\mathrm{k}} &= -\lambda \cdot m \cdot v \cdot \omega \cdot \frac{h_c}{d_w}, \\ W_{acc,\mathrm{k}} &= -\left|F_{in}\right| \cdot \frac{h_c}{2d_{cw}} = -m \cdot \left|\dot{v}\right| \cdot \frac{h_c}{2d_{cw}}, \end{aligned} \tag{25}$$

where W_{static} is the static weight on the wheel, g is gravitation acceleration, h_c is height of the mass center relative to the ground, d_{cw} is distance to castor wheels, and $W_{cf,\mathrm{k}}$ and $W_{acc,\mathrm{k}}$ are weighting forces due to centrifugal force and longitudinal acceleration, respectively. Positive/negative sign of the force $W_{cf,\mathrm{k}}$ means that it increases/decreases the static weight on the wheel. The force $W_{acc,\mathrm{k}}$ is always negative. The difference is that by acceleration the force acts on the rear castor wheel, while by deceleration it acts on the front castor wheel.

The weighting forces must remain positive at all times since otherwise the robot would tip over, i.e. $W_k > 0$. By substituting (18) and (19) into (25), considering the worst case where the weighting force decreases due to centrifugal acceleration, the following constraint is obtained:

$$-\frac{h_c}{2d_{cw}} \cdot \left|\ddot{s}\right| - \frac{h_c}{d_w} \cdot \left|\kappa(s)\right| \cdot \dot{s}^2 + \frac{g}{2} > 0, \tag{26}$$

which induces the following acceleration limits:

$$\begin{bmatrix} L_3(s,\dot{s}) \\ U_3(s,\dot{s}) \end{bmatrix} = \frac{2 \cdot d_{cw}}{h_c} \cdot \left(\frac{g}{2} - \frac{h_c}{d_w} \cdot \left|\kappa(s)\right| \cdot \dot{s}^2 \right) \cdot \begin{bmatrix} -1 \\ 1 \end{bmatrix}. \tag{27}$$

Using the Coulomb's friction model, the maximum force that can be developed between the wheel and the ground is

$$F_{fr,\mathrm{k}} = \mu \cdot W_k, \tag{28}$$

where μ is the friction coefficient.

By using (28), (25), (24) and (19) the condition (23) can be written as

$$\left[\frac{m}{2} \cdot \ddot{s} - \lambda \cdot \frac{J}{d_w} \left(\frac{d\kappa(s)}{ds} \cdot \dot{s}^2 + \kappa(s) \cdot \ddot{s} \right) \right]^2 + \frac{\left(m \cdot \kappa(s) \cdot \dot{s}^2 \right)^2}{4} \leq \left[\mu \cdot m \cdot \left(\frac{g}{2} - \lambda \cdot \frac{h_c}{d_w} \cdot \kappa(s) \cdot \dot{s}^2 - \frac{h_c}{2 \cdot d_{cw}} \cdot \left|\ddot{s}\right| \right) \right]^2. \tag{29}$$

Equation (29) can be written in the form of quadratic inequality:

$$\begin{aligned} & A(s,\dot{s}) \cdot \ddot{s}^2 + B(s,\dot{s}) \cdot \ddot{s} + C(s,\dot{s}) \leq 0, \\ & A(s,\dot{s}) = \left(\frac{m}{2} - \lambda \cdot \frac{J \cdot \kappa(s)}{d_w} \right)^2 - \left(\frac{\mu \cdot m \cdot h_c}{2 \cdot d_{cw}} \right)^2, \\ & B(s,\dot{s}) = \frac{-2 \cdot J}{d_w} \cdot \frac{d\kappa(s)}{ds} \left(\lambda \cdot \frac{m}{2} - \frac{J \cdot \kappa(s)}{d_w} \right) \cdot \dot{s}^2 + \\ & \qquad Q \cdot \frac{m^2 \cdot \mu^2 \cdot h_c}{d_{cw}} \cdot \left(\frac{g}{2} - \lambda \cdot \frac{h_c \cdot \kappa(s) \cdot \dot{s}^2}{d_w} \right), \\ & C(s,\dot{s}) = \left(\frac{J^2}{d_w^2} \cdot \left(\frac{d\kappa(s)}{ds} \right)^2 + \frac{m^2 \cdot \kappa(s)^2}{4} \right) \cdot \dot{s}^4 - \\ & \qquad m^2 \cdot \mu^2 \cdot \left(\frac{g}{2} - \lambda \frac{h_c \cdot \kappa(s) \cdot \dot{s}^2}{d_w} \right)^2, \end{aligned} \tag{30}$$

where $Q = 1$ in case $\ddot{s} \geq 0$ and $Q = -1$ in case $\ddot{s} < 0$. From (30) we get acceleration limits that prevent wheel slip for non-zero longitudinal velocity (note: $(s,\dot{s})$ is ommited for brevity)

$$\begin{bmatrix} L_{4,5} \\ U_{4,5} \end{bmatrix} = \frac{-B}{2A} + \frac{\sqrt{B^2 - 4AC}}{2A} \cdot \begin{bmatrix} -1 \\ 1 \end{bmatrix}, \tag{31}$$

where $L_4\big|_{Q=-1,\lambda=1}$ and $L_5\big|_{Q=-1,\lambda=-1}$ are lower acceleration limits for the left and for the right wheel, respectively, while $U_4\big|_{Q=1,\lambda=1}$ and $U_5\big|_{Q=1,\lambda=-1}$, are upper acceleration limits for the left and for the right wheel, respectively.

In case of pure rotation, s will denote the traversed angle, so that

$$v(t) = 0, \quad \omega(t) = \dot{s}(t), \quad \dot{v}(t) = 0, \quad \dot{\omega}(t) = \ddot{s}(t), \tag{32}$$

and dynamic model (19) is reduced to a single equation $\ddot{s} = \alpha$, from which we derive acceleration limits as

$$L_{1,rot}(s,\dot{s}) = \alpha_{min,rot}(s,\dot{s}),$$
$$U_{1,rot}(s,\dot{s}) = \alpha_{\max,rot}(s,\dot{s}),$$
$$\alpha_{min,rot}(s,\dot{s}) = \begin{cases} \bar{\alpha}_{min}, & \dot{s} \in [-\omega_{max}, \omega_{max}] \\ 0, & \text{otherwise} \end{cases}, \quad (33)$$
$$\alpha_{\max,rot}(s,\dot{s}) = \begin{cases} \bar{\alpha}_{\max}, & \dot{s} \in [-\omega_{max}, \omega_{max}] \\ 0, & \text{otherwise} \end{cases}.$$

To obtain limits for wheel slip prevention in case of pure rotation we first substitute (18) and than (32) into (29), which yields the condition for both wheels as

$$\frac{J}{d_w} \cdot |\ddot{s}| \le \frac{\mu \cdot m \cdot g}{2}, \quad (34)$$

which induces acceleration limits for pure rotation:

$$\begin{bmatrix} L_{2,rot}(s,\dot{s}) \\ U_{2,rot}(s,\dot{s}) \end{bmatrix} = \frac{\mu \cdot m \cdot g \cdot d_w}{2 \cdot J} \cdot \begin{bmatrix} -1 \\ 1 \end{bmatrix}. \quad (35)$$

Finally, overall acceleration limits are obtained using (16).

4. TIME-OPTIMAL VELOCITY PLANNING FOR STATIC FORMATIONS OF MOBILE ROBOTS

The problem of finding time-optimal trajectory along the predefined path of a static formation of mobile robots is defined as follows. For given predefined path $q(s):[0,s_g] \to CS$, initial state $(0,\dot{s}_0)$ and final state $(s_g,\dot{s}_g)$, find a monotonically increasing twice-differentiable time scaling function $s(t):[0,t_g] \to [0,s_g]$ that: (i) satisfies $s(0)=0$, $\dot{s}(0)=\dot{s}_0$, $s(t_g)=s_g$, $\dot{s}(t_g)=\dot{s}_g$, and (ii) minimizes total travel time t_g along the predefined path respecting actuator constraints, i.e. acceleration limits (16) for all mobile robots in the formation for all time $t \in [0,t_g]$.

To respect acceleration limits (16) of all mobile robots in the formation we have to map velocity $\dot{s}^i$ and acceleration $\ddot{s}^i$ of each mobile robot i in the formation to the reference path s.

In case of clothoid segments of the reference path, velocity for the i-th mobile robot is obtained from (10):

$$\dot{s}^i = \left(1 - r^i \cdot \kappa(s)\right) \cdot \dot{s}, \quad (36)$$

and its acceleration is obtained by differentiating (36),

$$\ddot{s}^i = -r^i \cdot \frac{d\kappa(s)}{ds} \cdot \dot{s}^2 + \left(1 - r^i \cdot \kappa(s)\right) \cdot \ddot{s}. \quad (37)$$

In case $p^i \neq 0$ path curvature $\kappa(s)$ in (36) and (37) becomes $\kappa(s) = \kappa(s + p^i)$, as can be seen in Fig. 2.

For straight part of reference path $\kappa(s)=0$ or for zero offset $r^i = 0$, velocity and acceleration of the i-th mobile robot in the formation are $\dot{s}^i = \dot{s}$ and $\ddot{s}^i = \ddot{s}$, respectively. From (36) follows that when the formation is turning (Fig. 1. b)), outside robots accelerate and inside robots decelerate to maintain formation, what one would naturally expect.

Let $L^i(s^i,\dot{s}^i)$ and $U^i(s^i,\dot{s}^i)$ denote minimum and maximum acceleration of the i-th robot along its path, respectively. Using (16) and (37) we get acceleration limits for the static formation of mobile robots

$$\max_{i=1,\dots,n_r} L^i(s,\dot{s}) \le \ddot{s} \le \min_{i=1,\dots,n_r} U^i(s,\dot{s}),$$
$$\begin{bmatrix} L^i(s,\dot{s}) \\ U^i(s,\dot{s}) \end{bmatrix} = \frac{1}{1 - r^i \cdot \kappa(s)} \cdot \left(\begin{bmatrix} L^i(s^i,\dot{s}^i) \\ U^i(s^i,\dot{s}^i) \end{bmatrix} + r^i \cdot \frac{d\kappa(s)}{ds} \cdot (\dot{s}^i)^2 \right), \quad (38)$$

where n_r is the total number of mobile robots in the formation.

Now we can address the problem of finding the time-optimal trajectory for static formation of mobile robots. The problem is best visualized in the $(s,\dot{s})$ phase plane (Fig. 4). The feasible acceleration constraint (38) can be illustrated as a cone of tangent vectors defined at any state $(s,\dot{s})$. The lower and upper edge of the cone corresponds to minimum and maximum acceleration, respectively. Actuation constraints (38) impose that there could be some states at which there is no feasible acceleration required for the system to continue to follow the path. This region is called inadmissible region (depicted in gray in Fig. 4), because one or more robots will leave the formation if its state is in this region. A switch from admissible region to inadmissible region occurs at the velocity limit curve $V(s)$.

For the i-th mobile robot, its velocity limit curve $V^i(s)$ satisfies

$$L^i(s^i,\dot{s}^i) = U^i(s^i,\dot{s}^i), \quad (38)$$

while for the formation it must be satisfied

$$\max_{i=1,\dots,n_r} L^i(s,\dot{s}) = \min_{i=1,\dots,n_r} U^i(s,\dot{s}). \quad (39)$$

To minimize travel time t_g, velocity $\dot{s}$ along the predefined path should be maximized, i.e. the area beneath the curve from initial state $(0,\dot{s}_0)$ to final state $(s_g,\dot{s}_g)$ should be maximized. This means that the curve always follows the upper or lower bound of the cone, i.e. the system always operates at minimum or maximum acceleration. The problem now reduces to finding the switching points between maximum and minimum accelerations.

The algorithm that gives sequence of values s where switching between maximum and minimum acceleration should occur, consists of the following steps [22] (see illustration in Fig. 4):

Step 1: Initialize switch counter $l=0$. Set $(s_l,\dot{s}_l) = (0,\dot{s}_0)$.

Step 2: Integrate equation $\ddot{s} = \max L^i(s,\dot{s})$ backward in time from $(s_g, \dot{s}_g)$ until the velocity limit curve is penetrated and call this phase plane curve F.

Step 3: Integrate equation $\ddot{s} = \min U^i(s,\dot{s})$ forward in time from $(s_l, \dot{s}_l)$. Call this curve A_l. Continue integrating until either A_l crosses F or A_l penetrates the velocity limit curve $V(s)$. If A_l crosses F, then add a new switch and the problem is solved. If instead the velocity limit curve $V(s)$ is penetrated in point $(s_{\lim}, \dot{s}_{\lim})$ proceed to Step 4.

Step 4: Search the velocity limit curve $V(s)$ forward from $(s_{\lim}, \dot{s}_{\lim})$ until the first local minimum of the velocity limit curve is found. Call that point $(s_{switch}, \dot{s}_{switch})$ and from this point integrate the curve $\ddot{s} = \max L^i(s,\dot{s})$ backward in time until it intersects A_l. Increment l and call this new curve A_l. Add intersection point as a new switch point from maximum to minimum acceleration.

Step 5: Increment l and set $(s_l, \dot{s}_l) = (s_{switch}, \dot{s}_{switch})$. Add another switch point at s_l and go to Step 3.

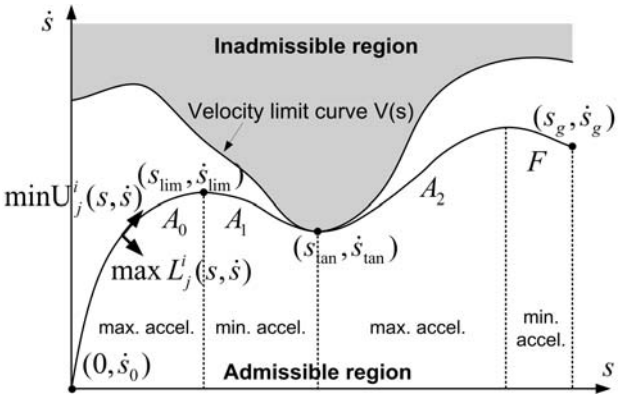

Fig. 4. An illustration of the optimal time-scaling algorithm.

When time-optimal velocity $\dot{s}$ along predefined path $q(s)$ is found it is possible to find velocity $\dot{s}^i$ for each mobile robot in the formation by applying (36).

5. EXPERIMENTAL RESULTS

The algorithm for finding the time-optimal trajectory for static formation of mobile robots is implemented in MATLAB®. One has to be careful in algorithm implementation, as many involved functions have discontinuities that make numerical integration prone to errors. Experiments were performed using robot soccer platform (Fig. 5). It consists of a team of five radio-controlled microrobots of size 7.5cm×7.5cm equipped with differential drive. The playground is of size 2.2m×1.8m. For postion tracking of the robots we mounted at 2.4 m height above the center of the playground the Basler a301fc IEEE-1394 digital color camera with resolution of 656×494 pixels and 80 fps framerate, and used the computer vision algorithm presented in [23].

The formation of four mobile robots at the start position and a predefined test path are shown in Fig. 6. The curvature profile of the test path is shown in Fig. 7. The robot R#1 is supposed to directly follow the test path without offset, while the offsets of mobile robots R#2, R#3 and R#4 with respect to the reference point are $[p^2\ r^2] = [0\ -0.35]$, $[p^3\ r^3] = [-0.15\ 0]$ and $[p^4\ r^4] = [-0.15\ -0.35]$, respectively. Orientation of each mobile robot in the formation at the start is 0°.

Fig. 5. Robot soccer platform.

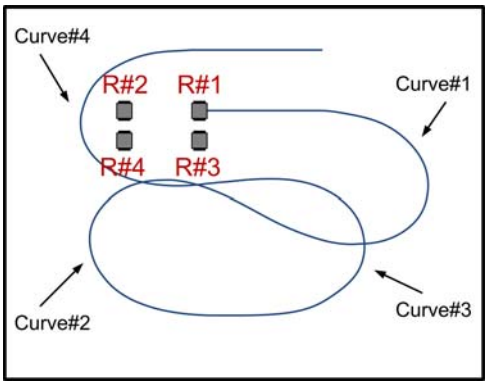

Fig. 6. Formation at the start position, and predefined path.

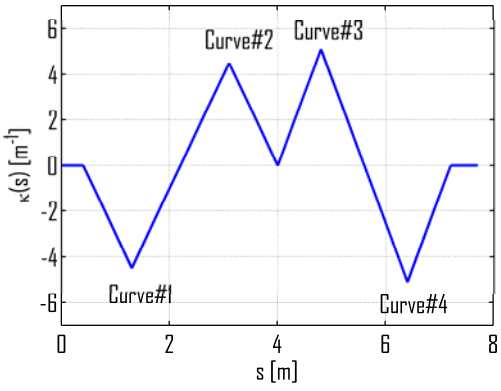

Fig. 7. Curvature profile of the predefined path.

In our experiment all mobile robots had the same parameters, but it is not a prerequisite and each robot can have different parameters. Mobile robot parameters used in experiment are given in Table 1. The parameters marked by a star are not mobile robots physical maximum values but are set as parameters in the robot firmware. Although robot soccer platform is very practical for experiments with formations of mobile

robots, it has some technical limitations that make driving at maximum accelerations impossible: (i) relatively large noise in the measured position and velocity of the robot; (ii) delay in the communication between the control computer and microprocessors of the mobile robots; (iii) delay in measurements due to vision (the time required to grab the image from the camera + time required for image processing); (iv) mobile robots allow only control of velocity (the internal controller in the mobile robot can generate higher torques than it was planned by the trajectory planner); (v) the trajectory tracking controller can also require higher torques than it was planned in order to compensate for trajectory tracking error. Because of this, it is necessary to choose more conservative parameters. Trajectories for each robot are planned offline using the proposed algorithm and then executed online using the nonlinear trajectory tracking controller presented in [24].

Table 1. Parameters of the mobile robot.

Parameter	Symbol	Value	Unit
Mass	m	0.4924	kg
Inertia moment	J	$4 \cdot 10^{-4}$	kg m^2
Min. long. accel. *	$\bar{a}_{\min}$	-1	m/s^2
Max. long. accel. *	$\bar{a}_{\max}$	1	m/s^2
Min. ang. accel. *	$\bar{\alpha}_{\min}$	-29.68	rad/s^2
Max. ang. accel. *	$\bar{\alpha}_{\max}$	22.32	rad/s^2
Max. long. velocity *	$\bar{v}_{\max}$	1.6	m/s
Max. ang. velocity *	$\bar{\omega}_{\max}$	12.8	rad/s
Friction coefficient	μ	0.4	-
Mass center height	h_c	0.025	m
Dist. between wheels	d_w	0.068	m
Dist. to castor wheels	d_{cw}	0.025	m
Gravitation	g	9.81	m/s^2

In Fig. 6 it can be seen that robots R#1 and R#3 enter the curve first (Curve #1). Since the robot R#1 is external (i.e. it has higher path radius), it is the one that resctricts the velocity of the formation in this curve. Therefore the first local minimum of the formation velocity in Fig. 9 is caused by the robot R#1. This can also be seen in Fig. 8 where its velocity profile touches its velocity limit curve. The robot R#2 is the next external robot that enters the curve (Curve #1) and restricts velocity of the formation. Therefore the second local minimum of the velocity in Fig. 9 is caused by the R#2, and in Fig. 8 the velocity profile of R#2 touches its velocity limit curve in that curve. Robots R#3 and R#4 do not limit the formation velocity here. Similarly, in the second curve (Curve #2) robot R#3 is external and since it enters the curve first (Curve #2), it restricts velocity of the formation, and after that the robot R#4 restricts velocity of the formation because it is the next external robot that enters the curve (Curve #2). Robots R#1 and R#2 do not restrict the velocity in the second curve (Curve #2). In the third curve (Curve #3) scenario is like in the second curve (Curve #2), while in the fourth curve (Curve #4) scenario is like in the first curve (Curve #1).

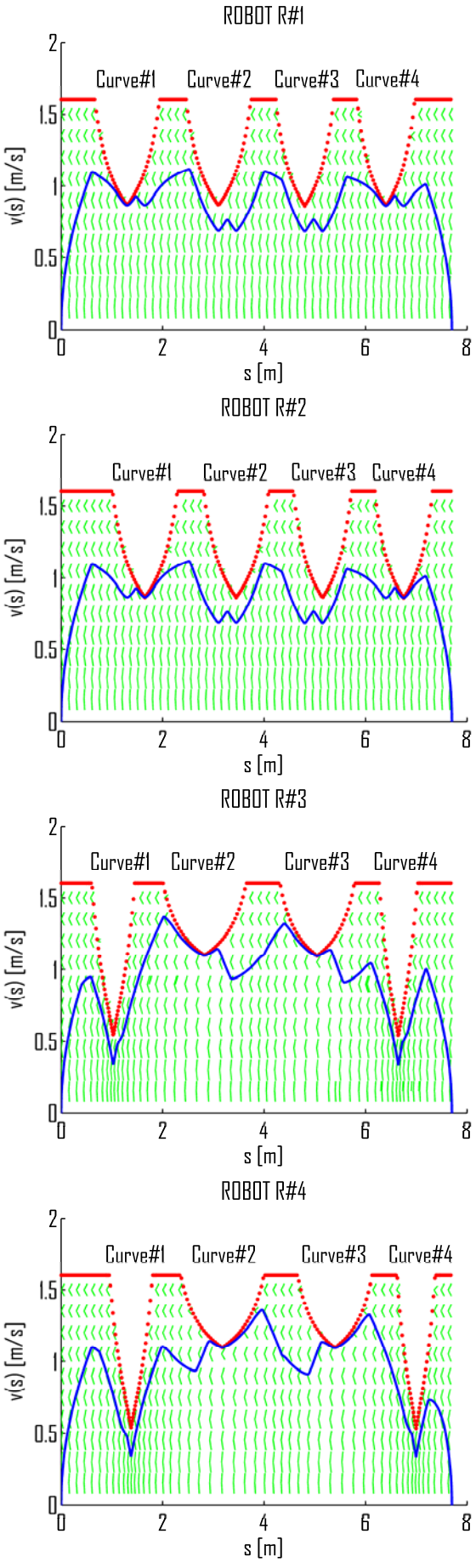

Fig. 8. Acceleration limits (cones), velocity limit curve (dot line) and time-optimal velocity (solid line) for all four mobile robots in the formation.

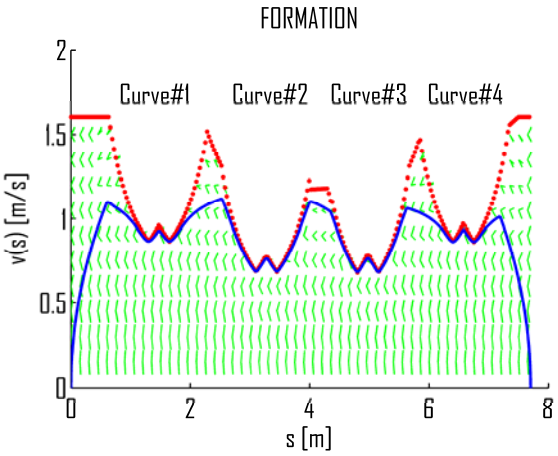

Fig. 9. Acceleration limits (cones), velocity limit curve (dot line) and time-optimal velocity (solid line) for the formation of mobile robots.

The paths of all four mobile robots in the formation are shown in Fig. 10. Obviously, the experiment confirmed that mobile robots in the formation are able to execute planned time-optimal velocity profiles.

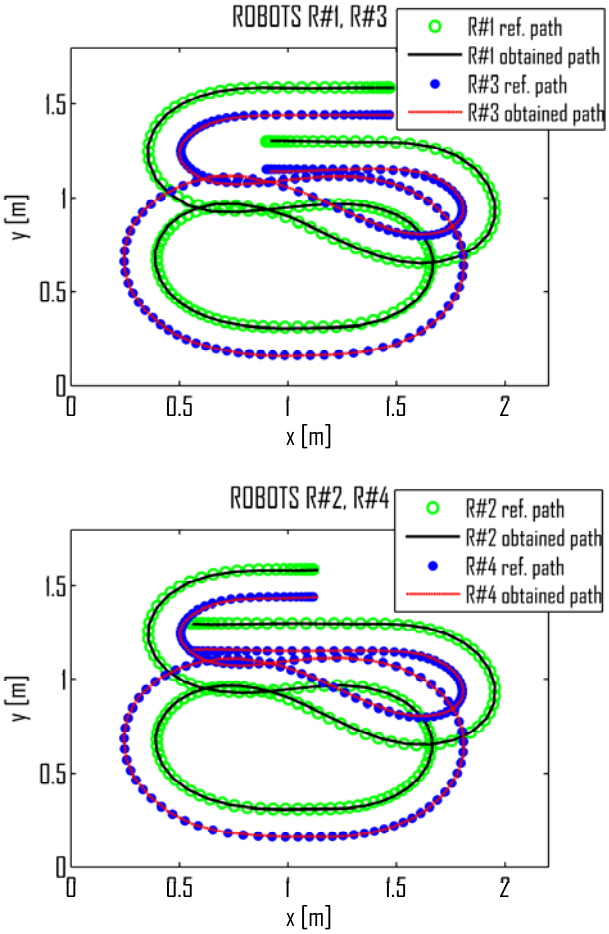

Fig. 10. Reference path and obtained mobile robot path.

6. CONCLUSION

The optimal time-scaling algorithm is developed for trajectory planning for the static formation of mobile robots along the predefined path with respect to velocity, acceleration, tip over and wheel slip prevention constraints of each mobile robot in the formation. A presented approach is very flexible and can be easily generalized for other types of robots and it can be extended to account for other constraints. In future work, we will try to extend this approach to the dynamic formations of mobile robots.

ACKNOWLEDGMENT

This research has been partly supported by the Ministry of Science, Education and Sports of the Republic of Croatia under the grant „Centre of Research Excellence for Data Science and Cooperative Systems“.

REFERENCES

[1] M. Dakulović and I. Petrović, “Two-way D* algorithm for path planning and replanning,” *Robotics and autonomous systems*, vol. 59, no. 5, pp. 329–342, May 2011.

[2] Y. Abbasi-Yadkori, J. Modayil, C. Szepesvari, “Extending rapidly-exploring random trees for asymptotically optimal anytime motion planning,” *International Conference on Intelligent Robots and Systems,* pp. 127-132, October 2010.

[3] G. Li, A. Yamashita, H. Asama, Y. Tamura, “An efficient improved artificial potential field based regression search method for robot path planning,” *International Conference on Mechatronics and Automation*, pp. 1227-1232, August 2012.

[4] M. Brezak and I. Petrović, “Real-time approximation of clothoids with bounded error for path planning applications,” *IEEE Transactions on Robotics*, vol. 30, no. 2, pp. 507-515, April 2014.

[5] T. Petrinić and I. Petrović, “A leader-follower approach to formation control of multiple non-holonomic mobile robots,” *Proceedings of MIPRO 2013 36th International Convention*, pp. 931-935, May 2013.

[6] K. G. Shin and N. D. McKay, “Minimum-time control of robot manipulators with geometric path constraints,” *IEEE Transaction on Automatic Control*, vol. 30, no. 6, pp. 531–541, July 1985.

[7] J. E. Bobrow, S. Dubowsky, and J. S. Gibson, “Time-optimal control of robotic manipulators along specified paths,” *The International Journal of Robotics Research*, vol. 4, no. 3, pp. 3-17, September 1985.

[8] K. Zhang, C.-M. Yuan, X.-S. Gao, “Efficient algorithm for time-optimal feedrate planning and smoothing with confined chord error and acceleration,” *The International Journal of Advanced Manufacturing Technology*, vol. 66, no. 9, pp. 1685-1697, June 2013.

[9] M. Lepetič, G. Klančar, I. Škrjanc, D. Matko, and B. Potočnik, “Time optimal path planning considering acceleration limits,” *Robotics and Autonomous Systems*, vol. 45, no. 3-4, pp. 199-210, December 2003.

[10] B. Lau, C. Sprunk, and W. Burgard, "Kinodynamic motion planning for mobile robots using splines," *IEEE/RSJ International Conference on Intelligent Robots and Systems*, pp. 2427-2433, October 2009.
[11] G. Lini, L. Consolini, and A. Piazzi, "Minimum-time constrained velocity planning," *17th Mediterranean Conference on Control and Automation*, pp. 748-753, June 2009.
[12] M. Brezak, *Localization, motion planning and control of mobile robots in intelligent spaces*. PhD thesis, University of Zagreb, Faculty of Electrical Engineering and Computing, 2010.
[13] Z. Shille and Y.-R. Gwo, "Dynamic motion planning of autonomous vehicles," *IEEE Transactions on Robotics and Automation*, vol. 7, no. 2, April 1991.
[14] M. Prado, A. Simon, E. Carabias, A. Perez, and F. Ezquerro, "Optimal velocity planning of wheeled mobile robots on specific paths in static and dynamic environments," *Journal of Robotic Systems*, vol. 20, no. 12, pp. 737-754, December 2003.
[15] Y. Huang, X. Zhang, Y. Fang, "Vision-based minimum-time planning of mobile robots with kinematic and visibility constraints," *Proceedings of the 19th International Federation of Automatic Control World Congress*, pp. 11878-11883, August 2014.
[16] P. F. Lima, M. Trincavelli, J. Martensson, B. Wahlberg, "Clothoid-Based Speed Profiler and Control for Autonomous Driving," *IEEE 18th International Conference on Intelligent Transportation Systems*, pp. 2194-2199, September 2015.
[17] L. Consolini, F. Morbidi, and D. Prattichizzo, "Stabilization of a hierarchical formation of unicycle robots with velocity and curvature constraints," *IEEE Transaction on Robotics*, vol. 25 no. 5, pp. 1176-1184, October 2009.
[18] L. Consolini, F. Morbidi, D. Prattichizzo, and M. Tosques, "Leader–follower formation control of nonholonomic mobile robots with input constraints," *Automatica*, vol. 44, no. 5, pp. 1343-1349, May 2008.
[19] T. D. Barfoot and C. M. Clark, "Motion planning for formations of mobile robots," *Robotics and Autonomous Systems*, vol. 46, no. 2, pp. 65-78, February 2004.
[20] http://en.wikipedia.org/wiki/Euler_spiral
[21] http://en.wikipedia.org/wiki/Parallel_curve
[22] H. Choset, K. M. Lynch, S. Hutchinson, G. Kantor, W. Burgard, L. E. Kavraki, and S. Thrun, *Principles of Robot Motion*, MIT Press, 2005.
[23] M. Brezak, I. Petrović, and E. Ivanjko, "Robust and accurate global vision system for real time tracking of multiple mobile robots," *Robotics and Autonomous Systems*, vol. 56, pp. 213-230, March 2008.
[24] M. Brezak, I. Petrović, and N. Perić, "Experimental comparison of trajectory tracking algorithms for nonholonomic mobile robots," *35th Annual Conference of the IEEE Industrial Electronics*, pp. 2229-2234, November 2009.

Toni Petrinić received B.Sc. degree in Electrical Engineering from the Faculty of Electrical Engineering and Computing (FER Zagreb), University of Zagreb, Croatia, in 2005. Since 2006 he has been with HEP-ODS d.o.o., Elektroprimorje Rijeka, Pogon Cres-Lošinj, where he is currently a head of technical department. His main research interest is in the field of mobile robotics.

Mišel Brezak received Ph.D degree in Electrical Engineering from the Faculty of Electrical Engineering and Computing (FER Zagreb), University of Zagreb, Croatia, in 2010. His main research interests are in the fields of mobile robotics and computer vision. He published 4 journal and more than 20 conference papers.

Ivan Petrović received B.Sc. degree in 1983, M.Sc. degree in 1989 and Ph.D. degree in 1998, all in Electrical Engineering from the Faculty of Electrical Engineering and Computing (FER Zagreb), University of Zagreb, Croatia. He had been employed as an R&D engineer at the Institute of Electrical Engineering of the Končar Corporation in Zagreb from 1985 to 1994. Since 1994 he has been with FER Zagreb, where he is currently a full professor. He teaches a number of undergraduate and graduate courses in the field of control systems and mobile robotics. His research interests include various advanced control strategies and their applications to control of complex systems and mobile robots navigation. He has published more than 40 journal and 160 conference papers, and results of his research have been implemented in several industrial products. He is a member of IEEE, IFAC – TC on Robotics and FIRA – Executive committee. He is a member of the Croatian Academy of Engineering.